

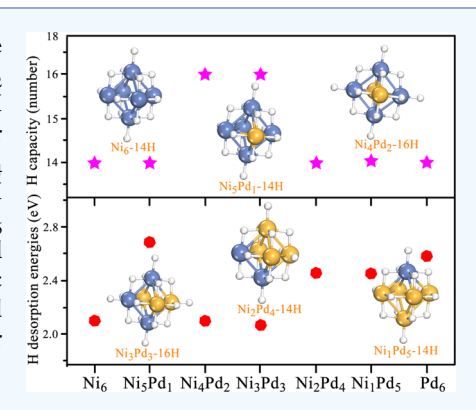


http://pubs.acs.org/journal/acsodf

Tuning the Catalytic Activity of Pd_xNi_y (x + y = 6) Bimetallic Clusters for Hydrogen Dissociative Chemisorption and Desorption

Shuangxiu Ma,[†] Shunxin Fei,[†] Liang Huang,*^{,†} Robert C. Forrey,*^{,§} and Hansong Cheng*^{,†}

ABSTRACT: Density functional theory was used to study dissociative chemisorption and desorption on Pd_xNi_y (x + y = 6) bimetallic clusters. The H_2 dissociative chemisorption energies and the H desorption energies at full H saturation were computed. It was found that bimetallic clusters tend to have higher chemisorption energy than pure clusters, and the capacity of Pd_3Ni_3 and Pd_2Ni_4 clusters to adsorb H atoms is substantially higher than that of other clusters. The H desorption energies of Pd_3Ni_3 and Pd_2Ni_4 are also lower than that of the Pd_6 cluster and comparable to that of the Ni_6 cluster, indicating that it is easier to pull the H atom out of these bimetallic catalysts. This suggests that the catalytic efficiency for specific Pd_xNi_y bimetallic clusters may be superior to bare Ni or Pd clusters and that it may be possible to tune bimetallic nanoparticles to obtain better catalytic performance.



INTRODUCTION

The catalyzed chemical reactions of transition metals are important industrial processes and have been studied both theoretically and experimentally for years. 1-4 Nickel family metals, including platinum, palladium, and nickel, are three of the most efficient catalysts. Palladium and platinum catalysts have been utilized in chemical processes such as reduction, hydrogenation, and oxidation. 5-13 The hydrides of nickel family metals have been used for applications in fuel cells, batteries, and hydrogen purifications, ¹⁴⁻¹⁷ and platinum is known to be an especially efficient catalyst for the hydrogen dissociation process.¹⁸ It is widely recognized that chemical reactions occur at the defect sites and sharp corners of catalysts, 19-21 and the size of the metal catalytic particles varies from nanoscale to mesoscale. 6,22,23 Many studies have demonstrated that nanosized catalytic particles are more chemically active than their corresponding bulk counterparts.

Single crystalline surface models at low H coverage have been employed to represent catalyst surfaces in many theoretical studies. ^{24,25} The structures of small metal clusters have been widely studied both experimentally ^{26–30} and theoretically. ^{31–39} Computationally, rigorous quantum mechanical modeling on Pd–Ni bimetallic catalyst nanoparticles with a realistic size is prohibitively difficult for the following reasons: (1) the catalyst nanoparticles usually contain thousands of atoms, (2) there are a large number of structural configurations for a given size of nanoparticle, and (3) there are numerous unpaired d-electrons in the nanoparticles. We thus choose a given size subnano cluster to represent the Pd–Ni bimetallic catalyst. Though such an unrealistically small

cluster size may not adequately represent the detailed structures and properties of an actual Pd–Ni catalyst nanoparticle, it does allow for a systematic study which may demonstrate the catalytic process well enough to provide useful insights into the mechanisms. Such a subnano cluster model has been shown to be capable of providing useful information on the catalytic properties. $^{13,40-42}$

The surface of a realistic catalyst is expected to be fully covered by either molecular or atomic hydrogen when the pressure is constantly maintained. Consequently, the catalytic performance of hydrogenation is critically dependent on how easily an H_2 molecule dissociates and how fast an H atom desorbs from a fully saturated surface. In our previous work of sequential H_2 dissociative chemisorption on small clusters, 45,51,53 we found that some of the most fundamental properties of catalytic particles (the dissociative chemisorption energy of H_2 and the desorption energy of H atoms at full H coverage) do not change significantly with particle size at full saturation of H atoms. Therefore, we perform density functional theory (DFT) calculations on H adsorption on Pd–Ni clusters at high coverage.

The hydride formation of small Pt, 45,46 Pd, 47-50,53 and Ni⁵¹ clusters has been systematically studied. The properties of the different metal clusters can vary considerably even within the same family of the periodic table, and the interactions between these metals and hydrogen may be considerably differ-

Received: May 10, 2019 Accepted: July 10, 2019 Published: July 23, 2019



[†]Sustainable Energy Laboratory, Faculty of Materials Science and Chemistry, China University of Geosciences (Wuhan), 388 Lumo Road, Wuhan 430074, PR China

[‡]The State Key Laboratory of Refractories and Metallurgy, Wuhan University of Science and Technology, No. 947 Heping Road, Wuhan 430081, PR China

⁸Department of Physics, Penn State University, Berks Campus, Reading, Pennsylvania 19610-6009, United States

ent.45-49,52 For example, the edge sites were identified as the most energetically favorable binding sites for H atoms on Ni clusters, 51 whereas both the hollow and edge sites are preferred on Pd clusters. 45,47-49,53 Another study indicated that the interaction between hydrogen and Pd clusters on nanoporous carbon materials can significantly enhance the H adsorption capacity of nanoporous carbon. 44 The hydride structures and vibrational spectra of Ni clusters calculated by Swart et al. 54 indicated that Ni clusters can accommodate more H atoms than other transition-metal clusters of the same size in the same row of the periodic table.⁵⁵ Additionally, the charge on the cluster can also influence the reactivity of the transitionmetal catalysts.⁵⁶ Although noble metal catalysts like Pt or Pd are highly active in the dissociative chemisorption and desorption processes, they are not substantial when compared to Ni and may not justify the higher cost associated with the limited availability of the precious metals. Furthermore, some studies have noted that the alloying design can be an effective method to improve the catalytic process. 40,57,58 Hence, the introduction of Ni into a pure Pd cluster may improve the catalytic performance and reduce the cost simultaneously.

In addition to the theoretical studies on monometallic clusters like Pt, Pd, and Ni mentioned above, there have been studies of some noble bimetallic clusters like Au/Pd^{43} and some bimetallic clusters of transition metals like Fe/Cr clusters and Al/Rh clusters. These studies mainly focus on the stability, electronic structures, and growth behavior. The selectivity of dehydrogenation of organic molecules on transition-metal oxides and nitrides suggested that the composition can influence both the activity and selectivity of catalysts. However, the processes of hydrogen adsorption and desorption on Pd_xNi_y bimetallic clusters with various compositions have not been systematically investigated.

In this paper, we conducted a systematic DFT study of hydride formation of small Pd_xNi_y bimetallic clusters at a given size (in the current study, x + y = 6), with the purpose of understanding the activity of the catalytic process of these clusters with H_2 . The key properties, including H_2 dissociative chemisorption energy, the barrier energy of migration of H atoms on the clusters, H atom desorption energy, and the maximum capacity for accommodating H atoms are systematically addressed. The findings in this study could provide useful insights into the catalytic performance of the bimetallic clusters of Ni family and shed light on the design of low-cost bimetallic nanoparticle catalysts.

Computational Details. All calculations were performed using DFT/generalized gradient approximation with the Perdew-Burke-Ernzerhof exchange-correlation functional as implemented in the DMol3 package. 65,66 The electronic structure calculations were carried out using a spin-polarization scheme to deal with the open-shell systems inherent to Ni and Pd atoms. A double numerical basis set augmented with polarization functions was used to describe the valence electrons and an effective core potential was employed to represent the core electrons, ^{67,68} as the valence electrons can determine the molecules' chemical properties and the basic functions in Dmol³ are numerically exact atomic orbitals rather than analytical functions. It has been shown that the quality of this basis set gives rise to very little superposition effects.⁶⁹ The Mulliken population division scheme was used to analyze the charge transfer between atoms.⁶⁹ The method used in the present study has been shown to be capable of providing accurate structures and cohesive energies of transition-metal

elements in good agreement with the available experimental values. 45,51,53 All structures were fully optimized without symmetry constraints, and the conjugated gradient algorithm was employed to search for energetically most stable structures. For the clusters with a given size, a thorough search for minimum energy structures was conducted. A DFT-D method of Tkatchenko and Scheffler⁷⁰ was tested in our calculations. We found that the influence of dispersion corrections on the final optimized structures and the energy change for chemisorption and desorption energies were negligible. The structure search for the transition state (TS) for H₂ on a Pd₃Ni₃ cluster was done to gain insight into the barriers of H₂ dissociative chemisorption kinetics and for H atom dispersal in the cluster using the linear synchronous transit/quadratic synchronous transit method. 71 The TS structure was verified by normal mode analysis that gives only one imaginary frequency.

The average formation energy ($\Delta E_{\rm FE}$) of a cluster containing x Pd and y Ni atoms can be calculated using

$$\Delta E_{\text{(FE)}} = [xE(Pd) + yE(Ni) - E(Pd_xNi_y)]/(x+y)$$
 (1)

where E(Ni) represents the energy of the Ni atom, E(Pd) represents the energy of the Pd atom, and $E(Ni_xPd_y)$ represents the energy of the clusters.

The dissociative chemisorption energy of H_2 and the desorption energy of H atoms at full H coverage are of vital importance for catalytic hydrogenation, as they determine how easily an H_2 molecule dissociates into and how fast an H atom desorbs from a fully H-saturated catalyst. The dissociative chemisorption energy of H_2 was calculated using the following equation

$$\Delta E_{(CE)} = 2[E(Pd_xNi_y) + n/2E(H_2) - E(Pd_xNi_yH_n)]/n$$
(2)

where *n* is the number of H atoms on the cluster, $E(Pd_xNi_yH_n)$ is the energy of the cluster with H atoms, and $E(H_2)$ is the energy of H_2 .

A realistic catalytic hydrogenation process is usually done at a hydrogen pressure that maintains full or nearly full coverage of the catalyst surfaces. Therefore, to evaluate the performance of a metallic catalyst, one needs to examine the hydrogen desorption energy from the cluster fully saturated by H. We note that H atoms are normally released sequentially rather than simultaneously. Hence, the dissociative chemisorption energy is not the energy required to desorb an H atom from the cluster. In the present study, we compared the desorption energies of different clusters fully saturated with H atoms using the following equation

$$\Delta E_{(DE)} = E_{(H)} - [E(Pd_xNi_yH_n) - E(Pd_xNi_yH_{n-2})]/2$$
(3)

where E(H) is the energy of the H atom and n represents the number of H atoms when the cluster is fully saturated.

To verify whether a cluster is fully covered by H atoms, we performed room-temperature ab initio molecular dynamics (AIMD) simulations on the clusters deemed to be saturated for 3 ps in an *NVT* canonical ensemble using the Nosé–Hoover thermostat^{72,73} for temperature control. Excessive H atoms on the clusters will recombine to form H₂ molecules weakly associated with the cluster upon the MD run.¹³

RESULTS AND DISCUSSION

The objective of the present study is to understand the catalytic properties of Pd/Ni bimetallic clusters with various compositions. Our previous study on bare Ni and Pd clusters indicated that when the cluster size is larger than six atoms, the change of the average formation energy is relatively small. Therefore, we chose Pd_xNi_y clusters that contain six atoms (x + y = 6) as a representative cluster model. For a given size of cluster, there are numerous isomeric configurations for the cluster structures with various compositions. To identify the lowest energy structure of a bare Pd_xNi_y cluster, we performed extensive structural optimizations to obtain the closest stable geometric configuration. Figure 1 shows the calculated lowest

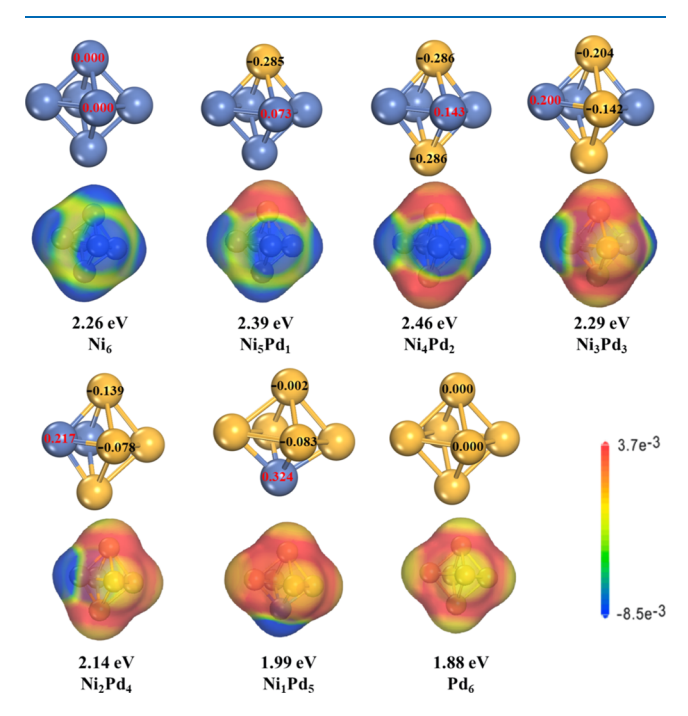


Figure 1. Optimized lowest energy geometries of the bare Pd_xNi_y clusters (x + y = 6) with Mulliken charge distribution, calculated electron density difference between a cluster and isolated atom, and the average formation energy.

energy structures with their average formation energies and the electron density difference of the clusters with different compositions. It reveals that the formation energy increases with the formation of Pd_xNi_y alloy clusters, and Ni₄Pd₂ possesses the highest formation energy. Therefore, Pd, Ni, bimetallic clusters are more stable than Ni₆ or Pd₆ monometallic clusters. The electron density difference and Mulliken charge analysis (as shown in Figure 1) indicate that the electron density of Pd atoms is higher than that of Ni atoms in Pd, Ni, bimetallic clusters because of the electron transfer from the Ni atoms to the neighboring Pd atoms, which is consistent with the fact that the electronegativity value of Ni (1.91) is relatively lower than that of Pd (2.20). As expected, the d-band center decreases gradually with the number of Pd atoms in Pd_xNi_y bimetallic clusters (-3.42 eV of Ni₆, -3.61 eV of Ni₅Pd, -3.69 eV of Ni₄Pd₂, -3.83 eV of Ni₃Pd₃, -4.00 eV of Ni₂Pd₄, -4.08 eV of NiPd₅, and -4.31 eV of Pd₆). The stability of Pd_xNi_v clusters and the charge distribution on Pd_xNi_y clusters may significantly influence their capability to interact with hydrogen.

The structures with the maximum formation energy of $\operatorname{Pd}_x\operatorname{Ni}_y$ clusters were chosen among their isomers for the study of H_2 chemisorption process. In the beginning of the chemisorption process, the H_2 molecule approaches the top sites of $\operatorname{Pd}_x\operatorname{Ni}_y$ clusters. Typically, there are two positions (Ni atom on the top sites and Pd atom on the top sites) that can accommodate the H_2 molecule. The calculated chemisorption structures of H_2 on $\operatorname{Pd}_x\operatorname{Ni}_y$ clusters with the lowest energy and their dissociative chemisorption energies are shown in Figure 2. The dissociative chemisorption energies changed with the

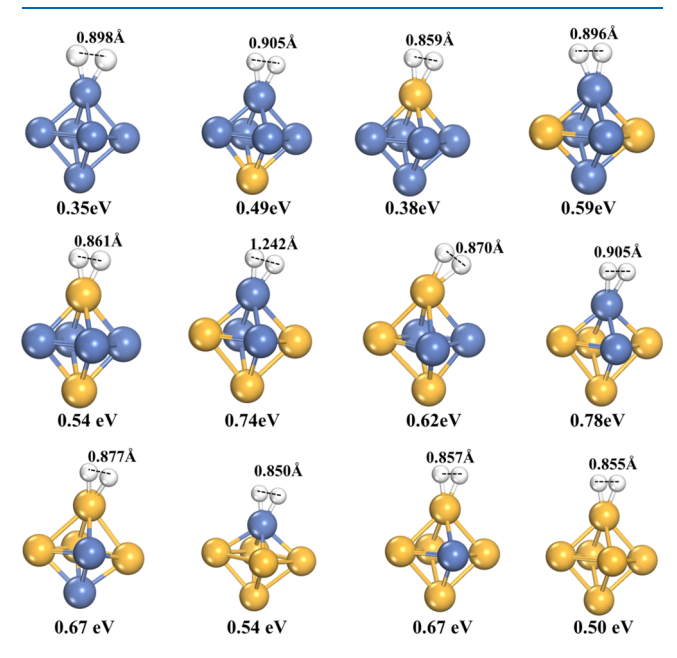


Figure 2. Calculated structures and chemisorption energies of Ni (blue) and Pd (yellow) top sites of different clusters.

compositions of $\operatorname{Pd}_x\operatorname{Ni}_y$ clusters. The bimetallic clusters tend to have higher chemisorption energies, suggesting that the bimetallic clusters are more readily able to absorb and dissociate H_2 than the pure Ni_6 or Pd_6 clusters.

Although the H₂ chemisorption on the top sites of Pd_rNi_v clusters is exothermic, it is not the most stable chemisorption configuration. The H atoms exhibit high mobility in the hydride complex, and they can easily diffuse to the twofold edge or threefold hollow sites. Figure 3 shows a detailed analysis of this process for an octahedral Pd₃Ni₃ cluster. Initially, the H₂ molecule approaches the cluster from the ontop site (R1) and undergoes dissociative chemisorption via the transition state (TS1) with a small barrier of 0.10 eV. This leads to H adsorption on two neighboring edges (P1) with an energy of -0.77 eV, which is the minimum energy structure for this octahedral cluster. However, the H atoms can further diffuse to other adsorption sites (e.g., from P1 to P2) with a relatively small barrier (TS2), indicating that H2 dissociative chemisorption and H diffusion processes are facile. A slightly larger barrier (TS3) between P2 and P3 is also shown in the figure. The small barrier of H2 dissociative chemisorption on bimetallic clusters and the highly favorable reaction energies show that this process is thermodynamically controlled, and the small diffusion barrier suggests that H migration on the bimetallic cluster of Ni family is facile.

The desorption energy of H on metal clusters at full saturation is a chemical quantity of vital importance, for it can

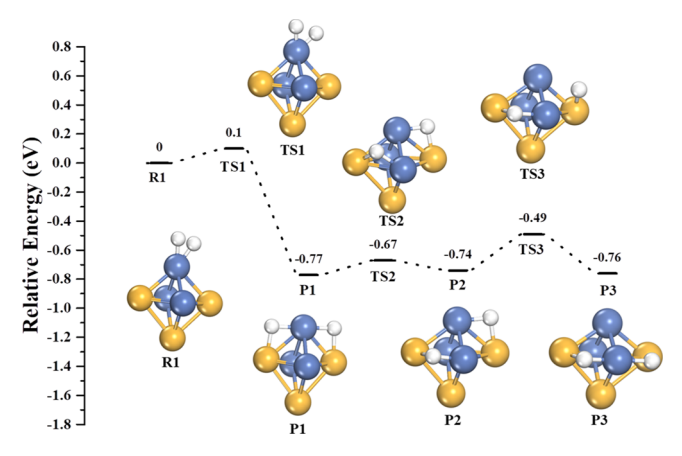


Figure 3. Calculated energy diagram of dissociative chemisorption of an H₂ molecule and the subsequent migration of the H atoms on the Pd₂Ni₂ octahedral cluster.

indicate the catalytic activity. Therefore, we considered the sequential loading of H_2 until the cluster is fully saturated with H atoms. In the process of H_2 dissociative chemisorption on the bimetallic metal cluster, the edge sites are populated at low H coverage. As the H loading increases, some hollow sites and on-top sites are also occupied. The saturation was checked by performing ab initio MD runs at 300 K to ensure that all the H atoms are chemisorbed. Figure 4 displays the radial

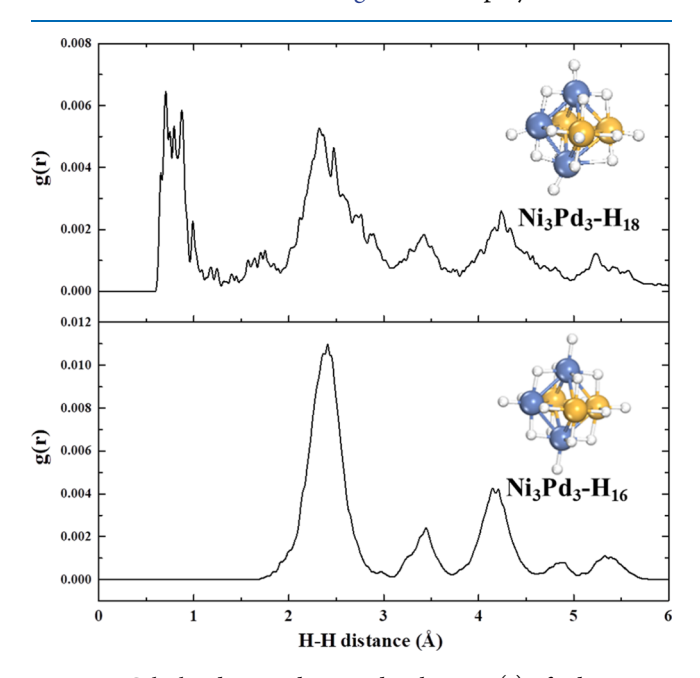


Figure 4. Calculated H–H distance distribution g(r) of $Pd_3Ni_3-H_{16}$ and $Pd_3Ni_3-H_{18}$ clusters. g(r) was obtained by tabulating all the H–H distances at each step of the AIMD trajectories fit with Gaussian functions.

distribution of the H–H distance of $Pd_3Ni_3-H_{16}$ and $Pd_3Ni_3-H_{18}$ clusters and shows that the H atoms in $Pd_3Ni_3-H_{16}$ are well separated by at least 2.0 Å. However, the top panel of the figure shows a peak at approximately 0.8 Å, indicating that an H_2 molecule was formed. Therefore, the saturation limit is 16 H atoms for this bimetallic cluster. To consider the entropic contributions and further verify the result of AIMD, we calculated the free energy for the formation of $Pd_3Ni_3-H_{16}$ ($Pd_3Ni_3+8H_2 \rightarrow Pd_3Ni_3-H_{16}$) and $Pd_3Ni_3-H_{18}$

(Pd₃Ni₃ + 9H₂ → Pd₃Ni₃−H₁₈) clusters at 300 K. The results showed that ΔG for the formation of Pd₃Ni₃−H₁₆ is −25.1 kcal/mol and that ΔG turned to a positive value (3.1 kcal/mol) when the loading of H atoms increased to 18, indicating that the Pd₃Ni₃ cluster is unable to absorb one more H₂ molecule spontaneously after reaching the maximum capacity. A previous study⁵¹ revealed that most of the Ni−H bond distances in Ni hydrides are between 1.6 and 1.7 Å, which are slightly shorter than the Pd−H bond distances (1.7−1.8 Å) in Pd hydrides. For the Pd_xNi_y bimetallic clusters that we studied, both the Pd−H and Ni−H bond distances are within the range of 1.6−1.8 Å, which is consistent with the pure Ni or Pd clusters.

The optimized structures of the fully H-saturated Pd_xNi_y clusters (x + y = 6) and desorption energies are shown in Figure 5. When the number of Pd atoms is high, the hollow

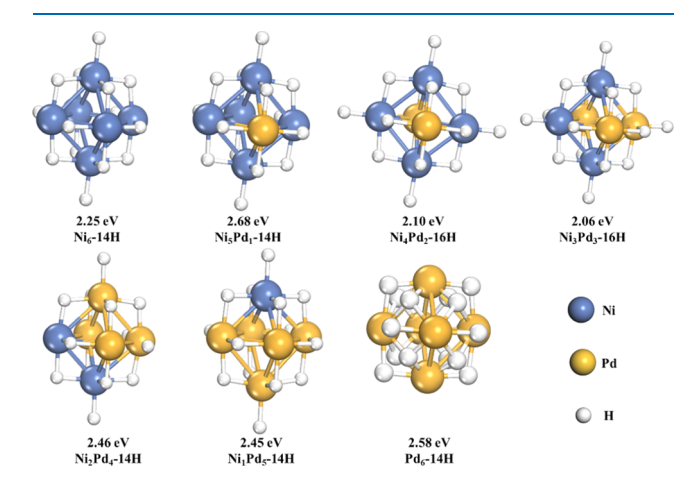


Figure 5. Optimized geometries of the fully saturated structures with minimum energies and the desorption energy when the first H atom was released.

sites are more favorable than the edge sites. With the increase of Ni atoms, the favorable sites change from the threefold hollow sites to the edge sites. When the number of Pd and Ni is close, the clusters (Pd_3Ni_3, Pd_2Ni_4) can load two more H atoms (n=16), compared to Ni_6 , Pd_6 , and other Pd_xNi_y clusters (n=14). After the 12 edges of the Pd_3Ni_3 and Pd_2Ni_4 clusters are occupied, there are four opposite on-top sites that are available for another four H atoms. It appears that the charge transfer from Ni atoms to the neighboring Pd atoms could make the on-top site load more H atoms.

The calculated maximum formation energy of clusters, the H₂ dissociative chemisorption energy, maximum H capacity, and the H desorption energy on Pd_xNi_y (x + y = 6) clusters are shown in Figure 6. The maximum formation energy of clusters reveals that the Pd_xNi_v alloy clusters possess higher formation energies than their pure cluster counterparts (Figure 6a), indicating they are more capable of maintaining their configuration when they undergo the sequential H₂ loading process. The H₂ dissociative chemisorption energies ΔE_{CE} vary in a small energy range from 0.35 to 0.78 eV. Figure 6b shows that Pd₃Ni₃ and Pd₄Ni₂ have higher H₂ dissociative chemisorption energies than other Pd_xNi_y clusters. Figure 6c shows the number of H atoms when the cluster is fully saturated. The Pd₃Ni₃ and Pd₂Ni₄ clusters can accommodate two more H atoms than the pure Pd and Ni clusters. The calculated H atom desorption energies $\Delta E_{(DE)}$ at full saturation

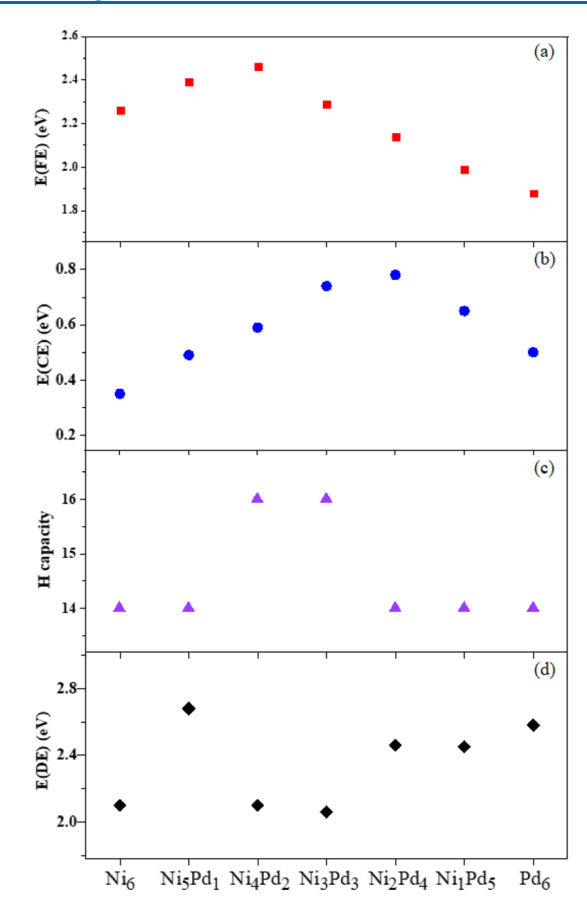


Figure 6. Comparison on (a) maximum formation energy, (b) H_2 dissociative chemisorption energy, (c) maximum H capacity, and (d) H desorption energy of small Ni, Pd, and Pd_xNi_y (x + y = 6) bimetallic clusters.

of the metal clusters vary within the range of 2.06-2.68 eV (Figure 6d). The highest H desorption energy is observed for Ni_5Pd_1 , which is slightly higher than other clusters. When the number of Pd and Ni atoms is similar, for example, Pd_3Ni_3 and Pd_2Ni_4 , the H desorption energies are lower than that of other clusters, indicating that it is easier to pull the H atom out of an appropriately tuned bimetallic catalyst. From the above analysis, we may conclude that bimetallic clusters with specific constitution (e.g., Pd_3Ni_3 and Pd_2Ni_4) have higher H_2 dissociative chemisorption energies, lower H desorption energy, and larger capacity of H atoms, which could lead to their better catalytic performance.

SUMMARY

We used DFT to study the chemical properties of subnano Pd_xNi_y bimetallic clusters for x+y=6. In general, bimetallic clusters have higher average formation energies and chemisorption energies than their pure cluster counterparts, which make them more stable and effective absorbers of hydrogen. The lower desorption energies make the H atoms facile to be pulled off from the surface of the clusters, which could lead to a higher catalytic activity for hydrogenation than that of the pure Pd or Ni clusters. The charge transfer from Ni to Pd increases the H capacity of Pd_3Ni_3 and Pd_2Ni_4 clusters by two atoms compared to pure Pd_6 and Ni_6 clusters. This represents a 14% increase for these bimetallic clusters, which is expected to scale with the cluster size. Our findings show that the bimetallic clusters can have better catalytic performance than

the pure clusters and may provide useful insights for tuning the component and interaction between the different metals in the design of alloy catalysts.

AUTHOR INFORMATION

Corresponding Authors

*E-mail: huangliang1986@wust.edu.cn (L.H.).

*E-mail: rcf6@psu.edu (R.C.F.).

*E-mail: chghs2@gmail.com (H.C.).

ORCID

Liang Huang: 0000-0001-7555-0021 Robert C. Forrey: 0000-0001-6687-5481

Notes

The authors declare no competing financial interest.

ACKNOWLEDGMENTS

We gratefully acknowledge support from the National Natural Science Foundation of China (nos. 51702241 and 21875225), the Natural Science Foundation of Hubei Province, China (no. 2017AAA126), and the United States National Science Foundation (no. PHY-1806180).

REFERENCES

- (1) Olsen, R. A.; Kroes, G. J.; Baerends, E. J. The influence of molecular rotation on the direct subsurface absorption of H2 on Pd(111). *J. Chem. Phys.* **1998**, *109*, 2450–2459.
- (2) Kresse, G. Dissociation and sticking ofH2on the Ni(111), (100), and (110) substrate. *Phys. Rev. B: Condens. Matter Mater. Phys.* **2000**, 62, 8295.
- (3) Horch, S.; Lorensen, H. T.; Helveg, S.; Lægsgaard, E.; Stensgaard, I.; Jacobsen, K. W.; Nørskov, J. K.; Besenbacher, F. Enhancement of Surface Self-Diffusion of Platinum Atoms by Adsorbed Hydrogen. *Nature* **1999**, 398, 134.
- (4) Wörz, A. S.; Judai, K.; Abbet, S.; Heiz, U. Cluster Size-Dependent Mechanisms of the CO + NO Reaction on Small Pdn(n≤ 30) Clusters on Oxide Surfaces. *J. Am. Chem. Soc.* **2003**, *125*, 7964.
- (5) Doyle, A. M.; Shaikhutdinov, S. K.; Jackson, S. D.; Freund, H.-J. Hydrogenation on Metal Surfaces: Why are Nanoparticles More Active than Single Crystals? *Angew. Chem., Int. Ed.* **2003**, 42, 5240–5243.
- (6) Heiz, U.; Sanchez, A.; Abbet, S.; Schneider, W.-D. Catalytic Oxidation of Carbon Monoxide on Monodispersed Platinum Clusters: Each Atom Counts. *J. Am. Chem. Soc.* **1999**, *121*, 3214–3217.
- (7) Pijper, E.; Kroes, G. J.; Olsen, R. A.; Baerends, E. J. Reactive and diffractive scattering of H2 from Pt(111) studied using a six-dimensional wave packet method. *J. Chem. Phys.* **2002**, *117*, 5885–5898
- (8) Podkolzin, S. G.; Alcalá, R.; Dumesic, J. A. Density functional theory studies of acetylene hydrogenation on clean, vinylidene- and ethylidyne-covered Pt(111) surfaces. *J. Mol. Catal. A: Chem.* **2004**, 218, 217–227.
- (9) Filhol, J.-S.; Neurock, M. Elucidation of the Electrochemical Activation of Water over Pd by First Principles. *Angew. Chem., Int. Ed.* **2006**, *45*, 402–406.
- (10) Wang, Y.; Balbuena, P. B. Roles of Proton and Electric Field in the Electroreduction of O2on Pt(111) Surfaces: Results of an Ab-Initio Molecular Dynamics Study. *J. Phys. Chem. B* **2004**, *108*, 4376–4384.
- (11) Hartnig, C.; Spohr, E. The role of water in the initial steps of methanol oxidation on Pt(111). *Chem. Phys.* **2005**, *319*, 185–191.
- (12) Ishikawa, Y.; Mateo, J. J.; Tryk, D. A.; Cabrera, C. R. Direct molecular dynamics and density-functional theoretical study of the electrochemical hydrogen oxidation reaction and underpotential deposition of H on Pt(111). *J. Electroanal. Chem.* **2007**, *607*, 37–46.

(13) Psofogiannakis, G.; St-Amant, A.; Ternan, M. Methane Oxidation Mechanism on Pt(111): A Cluster Model DFT Study. J. Phys. Chem. B 2006, 110, 24593–24605.

- (14) Cuevas, F.; Joubert, J.-M.; Latroche, M.; Percheron-Guégan, A. Intermetallic Compounds as Negative Electrodes of Ni/Mh Batteries. *Appl. Phys. A* **2001**, *72*, 225–238.
- (15) Chartouni, D.; Kuriyama, N.; Kiyobayashi, T.; Chen, J. Metal Hydride Fuel Cell with Intrinsic Capacity. *Int. J. Hydrogen Energy* **2002**, *27*, 945–952.
- (16) Lin, Y.; Rei, M.-H. Process Development for Generating High Purity Hydrogen by Using Supported Palladium Membrane Reactor as Steam Reformer. *Int. J. Hydrogen Energy* **2000**, *25*, 211–219.
- (17) Chen, S.; Hung, C.; Tu, G.; Rei, M. Perturbed hydrogen permeation of a hydrogen mixture-New phenomena in hydrogen permeation by Pd membrane. *Int. J. Hydrogen Energy* **2008**, 33, 1880–1880
- (18) Chen, L.; Zhou, C.-g.; Wu, J.-p.; Cheng, H.-s. Hydrogen adsorption and desorption on the Pt and Pd subnano clusters a review. *Front. Phys. China* **2009**, *4*, 356–366.
- (19) Liu, X.; Dilger, H.; Eichel, R. A.; Kunstmann, J.; Roduner, E. A Small Paramagnetic Platinum Cluster in an Nay Zeolite: Characterization and Hydrogen Adsorption and Desorption. *J. Phys. Chem. B* **2006**, *110*, 2013–2023.
- (20) Oudenhuijzen, M. K.; van Bokhoven, J. A.; Miller, J. T.; Ramaker, D. E.; Koningsberger, D. C. Three-Site Model for Hydrogen Adsorption on Supported Platinum Particles: Influence of Support Ionicity and Particle Size on the Hydrogen Coverage. *J. Am. Chem. Soc.* 2005, 127, 1530–1540.
- (21) Chaudhari, A.; Yan, C.-C. S.; Lee, S.-L. 2A + B2 →2AB catalytic reaction over rough surface: the effect of Eley-Rideal mechanism. *Catal. Today* **2004**, *97*, 89–92.
- (22) Visser, T.; Nijhuis, T. A.; Van Der Eerden, A. M. J.; Jenken, K.; Ji, Y.; Bras, W.; Nikitenko, S.; Ikeda, Y.; Lepage, M.; Weckhuysen, B. M. Promotion Effects in the Oxidation of Co over Zeolite-Supported Pt Nanoparticles. *J. Phys. Chem. B* **2005**, *109*, 3822–3831.
- (23) De Graaf, J.; Van Dillen, A. J.; De Jong, K. P.; Koningsberger, D. C. Preparation of Highly Dispersed Pt Particles in Zeolite Y with a Narrow Particle Size Distribution: Characterization by Hydrogen Chemisorption, Tem, Exafs Spectroscopy, and Particle Modeling. *J. Catal.* **2001**, 203, 307–321.
- (24) Papoian, G.; Nørskov, J. K.; Hoffmann, R. A Comparative Theoretical Study of the Hydrogen, Methyl, and Ethyl Chemisorption on the Pt(111) Surface. J. Am. Chem. Soc. 2000, 122, 4129–4144.
- (25) Busnengo, H. F.; Di Césare, M. A.; Dong, W.; Salin, A. Surface Temperature Effects in Dynamic Trapping Mediated Adsorption of Light Molecules on Metal Surfaces: H 2 on Pd (111) and Pd (110). *Phys. Rev. B: Condens. Matter Mater. Phys.* **2005**, 72, 125411.
- (26) Apsel, S. E.; Emmert, J. W.; Deng, J.; Bloomfield, L. A. Surface-Enhanced Magnetism in Nickel Clusters. *Phys. Rev. Lett.* **1996**, *76*, 1441.
- (27) Khanna, S.; Beltran, M.; Jena, P. Relationship between Photoelectron Spectroscopy and the Magnetic Moment of Ni 7 Clusters. *Phys. Rev. B: Condens. Matter Mater. Phys.* **2001**, *64*, 235419.
- (28) Liu, S.-R.; Zhai, H.-J.; Wang, L.-S. Sd Hybridization and Evolution of the Electronic and Magnetic Properties in Small Co and Ni Clusters. *Phys. Rev. B: Condens. Matter Mater. Phys.* **2002**, *65*, 113401.
- (29) Gerion, D.; Hirt, A.; Billas, I. M. L.; Châtelain, A.; de Heer, W. A. Experimental Specific Heat of Iron, Cobalt, and Nickel Clusters Studied in a Molecular Beam. *Phys. Rev. B: Condens. Matter Mater. Phys.* **2000**, *62*, 7491.
- (30) Knickelbein, M. B. Nickel Clusters: The Influence of Adsorbates on Magnetic Moments. *J. Chem. Phys.* **2002**, *116*, 9703–9711.
- (31) Alonso, J. A. Electronic and Atomic Structure, and Magnetism of Transition-Metal Clusters. *Chem. Rev.* **2000**, *100*, 637–678.
- (32) Estiu, G. L.; Zerner, M. C. Structural, Electronic, and Magnetic Properties of Small Ni Clusters. *J. Phys. Chem.* **1996**, *100*, 16874–16880.

- (33) Parks, E. K.; Zhu, L.; Ho, J.; Riley, S. J. The structure of small nickel clusters. I. Ni3-Ni15. *J. Chem. Phys.* **1994**, *100*, 7206–7222.
- (34) Reuse, F. A.; Khanna, S. N. Geometry, electronic structure, and magnetism of small Nin (n = 2-6, 8, 13) clusters. *Chem. Phys. Lett.* **1995**, 234, 77–81.
- (35) Desmarais, N.; Jamorski, C.; Reuse, F. A.; Khanna, S. N. Atomic Arrangements in Ni7 and Ni8 Clusters. *Chem. Phys. Lett.* **1998**, 294, 480–486.
- (36) Michelini, M. C.; Pis Diez, R.; Jubert, A. H. Density functional study of small Nin clusters, withn=2-6, 8, using the generalized gradient approximation. *Int. J. Quantum Chem.* **2001**, *85*, 22–33.
- (37) Michelini, M. C.; Pis Diez, R.; Jubert, A. H. Density functional study of the ionization potentials and electron affinities of small Nin clusters with n=2-6 and 8. *Comput. Mater. Sci.* **2004**, *31*, 292–298.
- (38) Baletto, F.; Ferrando, R. Structural Properties of Nanoclusters: Energetic, Thermodynamic, and Kinetic Effects. *Rev. Mod. Phys.* **2005**, 77. 371.
- (39) Futschek, T.; Hafner, J.; Marsman, M. Stable structural and magnetic isomers of small transition-metal clusters from the Ni group: anab initiodensity-functional study. *J. Phys.: Condens. Matter* **2006**, *18*, 9703.
- (40) Jia, M.; Vanbuel, J.; Ferrari, P.; Fernández, E. M.; Gewinner, S.; Schöllkopf, W.; Nguyen, M. T.; Fielicke, A.; Janssens, E. Size Dependent H2 Adsorption on AlnRh+ (n = 1-12) Clusters. *J. Phys. Chem. C* 2018, 122, 18247–18255.
- (41) Samadizadeh, M.; Peyghan, A. A.; Rastegar, S. F. DFT Studies of Hydrogen Adsorption and Dissociation on Mgo Nanotubes. *Main Group Chem.* **2016**, *15*, 107–116.
- (42) Yarovsky, I.; Goldberg, A. DFT study of hydrogen adsorption on Al13clusters. *Mol. Simul.* **2005**, *31*, 475–481.
- (43) Molina, L. M.; Benito, A.; Alonso, J. A. Ab Initio Studies of Ethanol Dehydrogenation at Binary Aupd Nanocatalysts. *Mol. Catal.* **2018**, *449*, 8–13.
- (44) Granja-DelRío, A.; Alonso, J. A.; López, M. J. Steric and chemical effects on the hydrogen adsorption and dissociation on free and graphene-supported palladium clusters. *Comput. Theor. Chem.* **2017**, *1107*, 23–29.
- (45) Zhou, C.; Wu, J.; Nie, A.; Forrey, R. C.; Tachibana, A.; Cheng, H. On the Sequential Hydrogen Dissociative Chemisorption on Small Platinum Clusters: A Density Functional Theory Study. *J. Phys. Chem. C* **2007**, *111*, 12773–12778.
- (46) Chen, L.; Cooper, A. C.; Pez, G. P.; Cheng, H. Density Functional Study of Sequential H2 Dissociative Chemisorption on a Pt6 Cluster. *J. Phys. Chem. C* **2007**, *111*, 5514–5519.
- (47) Bertani, V.; Cavallotti, C.; Masi, M.; Carrà, S. Density Functional Study of the Interaction of Palladium Clusters with Hydrogen and CHxSpecies. *J. Phys. Chem. A* **2000**, *104*, 11390–11397.
- (48) Roques, J.; Lacaze-Dufaure, C.; Mijoule, C. Dissociative Adsorption of Hydrogen and Oxygen on Palladium Clusters: A Comparison with the (111) Infinite Surface. *J. Chem. Theory Comput.* **2007**, 3, 878–884.
- (49) D'Anna, V.; Duca, D.; Ferrante, F.; La Manna, G. DFT Studies on Catalytic Properties of Isolated and Carbon Nanotube Supported Pd 9 Cluster—I: Adsorption, Fragmentation and Diffusion of Hydrogen. *Phys. Chem. Chem. Phys.* **2009**, *11*, 4077—4083.
- (50) Liu, X.; Tian, D.; Meng, C. Dft Study on the Adsorption and Dissociation of H2 on Pdn (N= 4, 6, 13, 19, 55) Clusters. *J. Mol. Struct.* **2015**, *1080*, 105–110.
- (51) Zhou, C.; Yao, S.; Zhang, Q.; Wu, J.; Yang, M.; Forrey, R. C.; Cheng, H. Hydrogen Sequential Dissociative Chemisorption on Ni $N(N = 2\sim9,13)$ Clusters: Comparison with Pt and Pd. *J. Mol. Model.* **2011**, *17*, 2305–2311.
- (52) Cheng, H.; Chen, L.; Cooper, A. C.; Sha, X.; Pez, G. P. Hydrogen Spillover in the Context of Hydrogen Storage Using Solid-State Materials. *Energy Environ. Sci.* **2008**, *1*, 338–354.
- (53) Zhou, C.; Yao, S.; Wu, J.; Forrey, R. C.; Chen, L.; Tachibana, A.; Cheng, H. Hydrogen Dissociative Chemisorption and Desorption

on Saturated Subnano Palladium Clusters (Pdn, N = 2-9). *Phys. Chem. Chem. Phys.* **2008**, *10*, 5445–5451.

- (54) Swart, I.; De Groot, F. M. F.; Weckhuysen, B. M.; Gruene, P.; Meijer, G.; Fielicke, A. H2Adsorption on 3d Transition Metal Clusters: A Combined Infrared Spectroscopy and Density Functional Study. *J. Phys. Chem. A* **2008**, *112*, 1139–1149.
- (55) Ashman, C.; Khanna, S. N.; Pederson, M. R. Hydrogen Absorption and Magnetic Moment of Nin Clusters. *Chem. Phys. Lett.* **2003**, 368, 257–261.
- (56) Huang, L.; Han, B.; Xi, Y.; Forrey, R. C.; Cheng, H. Influence of Charge on the Reactivity of Supported Heterogeneous Transition Metal Catalysts. *ACS Catal.* **2015**, *5*, 4592–4597.
- (57) Samin, A. J.; Andersson, D. A.; Holby, E. F.; Uberuaga, B. P. First-Principles Localized Cluster Expansion Study of the Kinetics of Hydrogen Diffusion in Homogeneous and Heterogeneous Fe-Cr Alloys. *Phys. Rev. B: Condens. Matter Mater. Phys.* **2019**, 99, 014110.
- (58) Carneiro, J. W. d. M.; Cruz, M. T. d. M. Density Functional Theory Study of the Adsorption of Formaldehyde on Pd4 and on Pd4/Γ-Al2o3 Clusters. *J. Phys. Chem. A* **2008**, *112*, 8929–8937.
- (59) Frank, H.; Joseph, W.; McGregor, D.; López, G. E. The Electronic Structures of Nickel-Palladium Alloy Clusters: A Density Functional Theory Study. *Chem. Lett.* **2018**, *47*, 458–460.
- (60) Sosa-Hernández, É. M.; Montejano-Carrizales, J. M.; Alvarado-Leyva, P. G. Global Minimum Structures, Stability and Electronic Properties of Small Ni X Sn Y ($X+Y \le 5$) Bimetallic Clusters; a Dft Study. Eur. Phys. J. D **2016**, 70, 208.
- (61) Singh, R. K.; Iwasa, T.; Taketsugu, T. Insights into geometries, stabilities, electronic structures, reactivity descriptors, and magnetic properties of bimetallic Ni m Cu n-m (m = 1, 2; n = 3-13) clusters: Comparison with pure copper clusters. *J. Comput. Chem.* **2018**, 39, 1878–1889.
- (62) Benaida, M.; Aiadi, K.; Mahtout, S.; Djaadi, S.; Rammal, W.; Harb, M. Growth Behavior and Electronic Properties of Ge N+ 1 and Asge N (N= 1–20) Clusters: A Dft Study. *J. Semicond.* **2019**, *40*, 032101.
- (63) Miran, H. A.; Altarawneh, M.; Jiang, Z.-T.; Oskierski, H.; Almatarneh, M.; Dlugogorski, B. Z. Decomposition of Selected Chlorinated Volatile Organic Compounds by Ceria (Ceo2). *Catal. Sci. Technol.* **2017**, *7*, 3902–3919.
- (64) Jaf, Z. N.; Altarawneh, M.; Miran, H. A.; Jiang, Z.-T.; Dlugogorski, B. Z. Mechanisms governing selective hydrogenation of acetylene over γ -Mo2N surfaces. *Catal. Sci. Technol.* **2017**, 7, 943–960
- (65) Delley, B. Fast Calculation of Electrostatics in Crystals and Large Molecules. J. Phys. Chem. A 1996, 100, 6107–6110.
- (66) Delley, B. From molecules to solids with the DMol3 approach. J. Chem. Phys. 2000, 113, 7756–7764.
- (67) Dolg, M.; Wedig, U.; Stoll, H.; Preuss, H. Energy-adjust-edabinitiopseudopotentials for the first row transition elements. *J. Chem. Phys.* **1987**, *86*, 866–872.
- (68) Bergner, A.; Dolg, M.; Küchle, W.; Stoll, H.; Preuß, H. Ab initio energy-adjusted pseudopotentials for elements of groups 13-17. *Mol. Phys.* **1993**, *80*, 1431–1441.
- (69) Delley, B. An all-electron numerical method for solving the local density functional for polyatomic molecules. *J. Chem. Phys.* **1990**, 92, 508–517.
- (70) Tkatchenko, A.; Scheffler, M. Accurate Molecular Van Der Waals Interactions from Ground-State Electron Density and Free-Atom Reference Data. *Phys. Rev. Lett.* **2009**, *102*, 073005.
- (71) Halgren, T. A.; Lipscomb, W. N. The Synchronous-Transit Method for Determining Reaction Pathways and Locating Molecular Transition States. *Chem. Phys. Lett.* **1977**, 49, 225–232.
- (72) Nosé, S. A Unified Formulation of the Constant Temperature Molecular Dynamics Methods. *J. Chem. Phys.* **1984**, *81*, 511–519.
- (73) Martyna, G. J.; Tuckerman, M. E.; Tobias, D. J.; Klein, M. L. Explicit Reversible Integrators for Extended Systems Dynamics. *Mol. Phys.* **1996**, *87*, 1117–1157.